# Light-driven hydrogen production with CdSe quantum dots and a cobalt glutathione catalyst

| | |
|---|---|
| Journal: | *ChemComm* |
| Manuscript ID | CC-COM-11-2020-007364.R1 |
| Article Type: | Communication |
| | |

COMMUNICATION

# Light-driven hydrogen production with CdSe quantum dots and a cobalt glutathione catalyst

Received 00th January 20xx,
Accepted 00th January 20xx

DOI: 10.1039/x0xx00000x

Rebeckah Burke[a†], Saikat Chakraborty[a†], Kevin P. McClelland[a], Jana Jelušić[a], Ellen M. Matson[a], Kara L. Bren[a]*, and Todd D. Krauss[a,b]*

**A photocatalytic hydrogen ($H_2$) production system is reported using glutathione (GSH)-capped CdSe QDs with a cobalt precatalyst, yielding 130,000 mol $H_2$ per mol cobalt over 48 hours. Analysis of the reaction mixtures after catalysis indicates that the active catalyst is a labile complex of cobalt and GSH formed *in situ*.**

Hydrogen ($H_2$), an energy-dense and clean-burning fuel, is an alternative to fossil fuels that is generated in the reductive half-reaction of water splitting.[1, 2] Systems capable of photocatalytic $H_2$ generation typically include a photosensitizer, catalyst, and sacrificial electron donor (Figure 1). Colloidal semiconducting nanocrystal quantum dots (QDs) are appealing photosensitizing materials owing to their size-tuneable reduction and oxidation potentials,[3] large absorption cross sections with broad absorption across the visible spectrum,[4] and superior photostability as compared to molecular dyes.[5, 6]

Heterostructures with QDs and attached catalytic metal nanoparticles have gained interest for light-driven proton reduction, but frequently involve the use of noble metals as catalytically active sites.[7, 8] Alternate approaches have utilized small molecules,[9-12] hydrogenase enzymes,[13] or simple metal salts[6, 14, 15] as catalytic partners with QD photosensitizers. In this regard, cobalt has received much attention as it is more abundant than noble metals and, in combination with appropriate ligands, has been found to efficiently facilitate the reduction of protons to $H_2$.[11, 12, 16] Indeed, molecular cobalt-based catalysts have been studied with CdSe QD photosensitizers for $H_2$ production.[9-12] With QDs, some of these catalysts have maintained stable activity,[9, 10] while others have lasted <10 hours.[11, 12] The cases with low efficiency could be partially explained by ligands dissociating from the QD and binding to the cobalt complex, poisoning the catalyst.[9]

A simple method to avoid deleterious reactivity toward molecular catalysts by dissociated QD ligands is to add metal salts to the solution to form catalytically active complexes *in situ*.[6, 9] This strategy has been applied for other metals. For example, combination of $Ni^{2+}$ with dihydrolipoic acid (DHLA)-capped CdSe QDs formed an active Ni-DHLA catalyst and achieved high photocatalytic activity (600,000 mol $H_2$ formed per mol Ni).[6] Simple cobalt salts have also been used as precatalysts in QD-based photocatalytic systems, resulting in TONs approaching 60,000 (mol $H_2$ per mol Co).[14, 15] In both cases, cobalt attached to the QD surface, causing QD

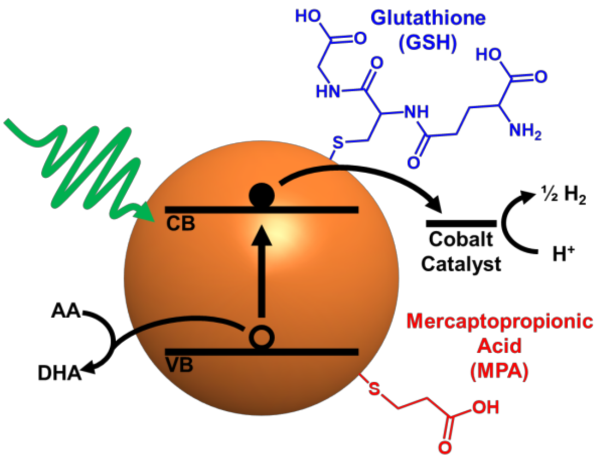

**Figure 1.** Illustration of photocatalytic proton reduction with CdSe QDs capped with glutathione (GSH) or mercaptopropionic acid (MPA). Upon excitation by visible light, the QD transfers an electron to a cobalt co-catalyst in solution which reduces protons to form $H_2$. Finally, the photogenerated holes are transferred to the sacrificial reductant, ascorbic acid (AA), reestablishing the QDs.

---

[a] *Department of Chemistry, University of Rochester, Rochester, New York 14627, USA.*
[b] *The Institute of Optics, University of Rochester, Rochester, New York, 14627 USA.*
† Denotes authors contributed equally to this work.

Electronic Supplementary Information (ESI) available: Sample preparation and characterization, experimental details for photocatalytic H2 production and redispersion experiments, calculation of external QY for H2 production, ICP-MS sample preparation and experimental details, characterization of as-synthesized CdSe QDs, TEM micrographs for CdSe-GSH QDs, photocatalytic H2 generation with CdSe-GSH and CoCl2 over 91 hours, illustration of the photocatalytic redispersion experiment with corresponding $H_2$ generation over time and a table describing the experimental conditions and results, brightfield TEM micrographs and EDX spectrum of CdSe-GSH QDs after photocatalysis with CoCl2 with a table including corresponding weight percent values, Co and Cd concentrations as determined from ICP-MS. See DOI: 10.1039/x0xx00000x aggregation and precipitation of the catalytic species.[14, 15] Importantly, these reports did not observe ligation of the capping ligands to the $Co^{2+}$, and high photocatalytic activity was reported only when the QD capping ligands were completely removed.[14, 15] As such, an investigation into possible active catalysts formed *in situ* between thiolate ligands and cobalt ions is needed.

Toward this goal, samples of water-soluble CdSe QDs were prepared using either glutathione (GSH) or mercaptopropionic acid (MPA) capping ligands (Figure 1, details of QD preparation and characterization are in Supporting Information). Two QD-ligand systems were studied here to show that *in situ* catalyst formation is not limited to one specific ligand and to determine the impact of ligand functional groups on catalyst activity. Specifically, GSH was selected as a potentially multidentate tripeptide ligand, while MPA, a common QD ligand, was chosen as it also contains thiol and carboxylic acid moieties but does not have the amine and amide groups found in GSH.[12, 13] After ligand exchange, CdSe-GSH and CdSe-MPA QDs exhibit similar absorption spectra with first exciton absorbance transitions centred at 533 ± 5 nm (Figure S2). Transmission electron microscopy (TEM) confirms that the size of the QDs remains largely unchanged following ligand exchange (Figure S2).

Systems for photocatalytic $H_2$ production were prepared with the addition of a cobalt salt precatalyst (1 μM $CoCl_2$) and ascorbic acid (0.5 M AA) as an electron donor to 1 μM QDs in water at pH 4.5. Over 48 hours, samples containing both CdSe-GSH QDs and $CoCl_2$ exhibited significantly higher $H_2$ production activity (650 ± 160 μmol $H_2$) than samples lacking $CoCl_2$ (270 ± 80 μmol $H_2$) (Figure 2). The corresponding TON, on average, was 130,000 ± 30,000 mol $H_2$ per mol $Co^{2+}$, with a quantum yield (QY) of 28 ± 5%. $H_2$ production was observed continuously for 91 h, resulting in an overall TON of ~210,000 with respect to $Co^{2+}$ (Figure S3). Comparing these results to CdSe-MPA, we observed a decrease in total $H_2$ produced with MPA-coated QDs without $CoCl_2$ (170 ± 70 μmol). These results are consistent with our previous findings which showed that CdSe-GSH is a better sole photocatalyst than CdSe-MPA.[17] While CdSe-MPA also showed a large enhancement in $H_2$ production with the addition of the cobalt salt (350 ± 100 μmol) (Figure 2a), the yield of $H_2$ was only half of what was produced by the system with cobalt and CdSe-GSH.

As the yield of $H_2$ is improved in the presence of $CoCl_2$ as compared to QDs alone, we sought to better understand the role and speciation of this metal ion under catalytic conditions. Three possible interactions between $Co^{2+}$ and QDs, responsible for increased catalytic activity, were considered: (1) metal cation substitution at the QD surface, (2) metal cations coordinated to the surface capping ligands bound to the QD, or (3) *in situ* formation of a freely-diffusing cobalt-containing catalyst generated upon coordination of the transition metal to GSH ligands dissociated from the QD surface (Figure S4). To determine whether cobalt ions associate with the surface of the CdSe-GSH QDs, both TEM and energy dispersive X-ray (EDX) spectroscopy analyses were used to examine the nanocrystals following photocatalysis and precipitation of the QDs via centrifugation (Figure S5 and Table S1). While there is evidence of QD agglomeration following irradiation, no cobalt deposition was observed on the QD surface. However, given the low concentration of $Co^{2+}$ used in these photocatalytic reactions, we further analysed the CdSe-GSH QDs following catalysis via inductively coupled plasma-mass spectrometry (ICP-MS), as described in Supporting Information. Analysis of both the supernatant solution and precipitated QDs revealed that over 97% of the total cobalt was present in the solution, while 98% of all cadmium was detected in the pellet (Table S2).

To further assess whether cobalt irreversibly binds to the surface of the CdSe-GSH QDs during photocatalysis, a mixture of the nanocrystals, $CoCl_2$, and AA was irradiated for 48 hours. Subsequently, the CdSe-GSH QDs were precipitated via centrifugation (Figure S6 and Table S3 for a schematic of the experiment and table of results). The QD pellet was redispersed in water with fresh AA, and upon re-irradiation of the recycled QDs, a significantly decreased volume of $H_2$ was formed over 48 h (82 ± 15 μmol $H_2$). Notably, this level of activity is the same as for fresh QDs alone (98 ± 8 μmol; Figure S3). The similarity in activity of the pellet to that of the QD-only case suggests that $H_2$ production activity is not a result of $Co^{2+}$ strongly associating with the surface of the QDs. Indeed, upon addition of $CoCl_2$ to

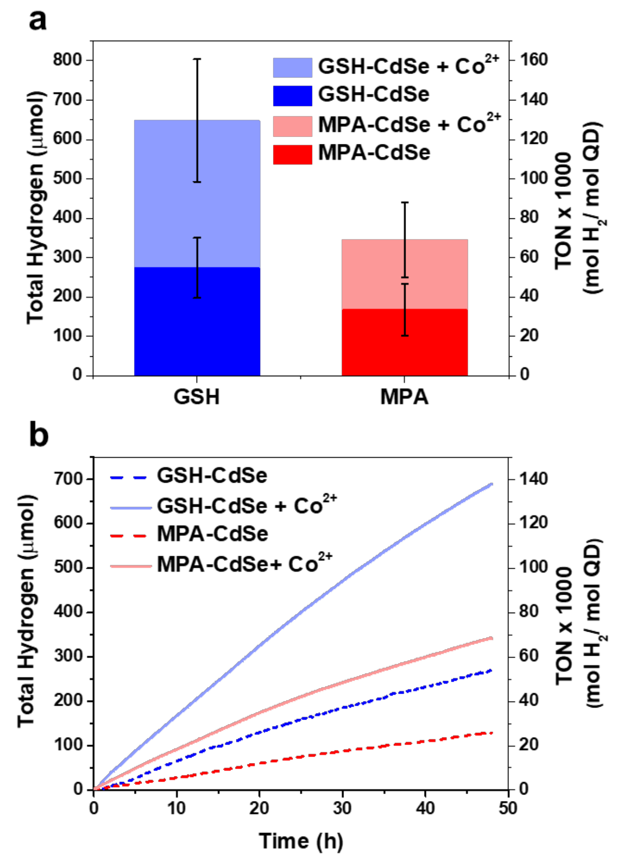

**Figure 2.** (a) Average $H_2$ evolution and corresponding TONs for 1 μM CdSe-GSH (blue) or CdSe-MPA (red) with 0.5 M AA, pH 4.5 after 48 hours of illumination ($\lambda_{ex}$=525 nm) either with (light) or without (dark) 1 μM $CoCl_2$. Error bars were determined by the standard deviation of 10 measurements. (b) Representative plots of photocatalytic $H_2$ production over time under the same experimental conditions as in (a).

the redispersed QDs, the activity of the photocatalytic system was restored (Table S3, Figure S7).

Similar experiments were used to probe photochemical $H_2$ production from the supernatant. While no $H_2$ production was observed from the solvated species separated from the QD pellet, addition of fresh CdSe-GSH QDs to the supernatant restored $H_2$ production to the otherwise inactive mixture (Figure S7). Taken altogether, these data support the hypothesis that a freely-diffusing cobalt catalyst is formed in solution, and not directly bound to the surface of the CdSe-GSH QDs.

We propose that the active catalyst formed *in situ* consists of one or more soluble molecular species generated via coordination of cobalt to GSH ligands that dissociated from CdSe QDs (Figure S4). To test this hypothesis, we examined an *ex situ* complex of cobalt and GSH in the absence of QDs. Upon combining $CoCl_2$ and GSH in a 1:2 molar ratio at pH 4.5, a brown product, denoted $Co_x(GSH)_y$, is formed. The mixture displays absorption maxima at ~390 and ~460 nm with a shoulder at ~320 nm (Figure 3a, dark blue curve). Similar absorption bands have been reported for complexes of cobalt and cysteine,[18, 19] as well as cobalt and MPA,[20] and are attributed to ligand-field bands in mononuclear or binuclear Co(III) complexes with S, O, and/or N (for cysteine) coordination to cobalt. We note that that, while these absorption bands are not seen with $CoCl_2$ and AA alone (Figure 3a, green curve), we do not know if AA played an assisting role in the formation of $Co_x(GSH)_y$.

To determine whether $Co_x(GSH)_y$ catalyses $H_2$ production, we collected its cyclic voltammogram (CV) and performed constant potential electrolysis (CPE) measurements (Figures S8 and S9). The CV reveals an irreversible wave with an onset potential of ~ –0.9 V vs. Ag/AgCl (1 M KCl), consistent with proton reduction (Figure 3b, dark blue curve). This feature is not observed in the samples of $CoCl_2$ or GSH. This result is consistent with the formation of a $Co_x(GSH)_y$ species that is responsible for the catalytic $H_2$ production. Importantly, this onset potential is anodic of previously reported conduction band potentials (-1.2 V vs. Ag/AgCl) for CdSe QDs of a similar size, supporting our hypothesis that electron transfer from the QD to $Co_x(GSH)_y$ is thermodynamically favorable.[3, 6, 21] Illumination of $CoCl_2$, AA, and GSH without QDs shows no measurable $H_2$ production and further support that the photogenerated electrons come from the QD (Table S5).

In an attempt to isolate and characterize the catalytically active $Co_x(GSH)_y$ complex, we subjected the sample to size-exclusion chromatography. Fractions (1-mL), each with distinct absorption spectra (Figure 3a) and CVs (Figure 3b), were collected. The first fraction exhibits absorption features similar to the crude mixture of $CoCl_2$ and GSH, and electrochemical analysis revealed an irreversible reduction event consistent with $H_2$ evolution. However, this feature is shifted cathodically from that observed for the crude sample. Subsequent fractions show minimal activity by CV and weaker absorption features.

Size-exclusion chromatography is a gentle separation technique. Nevertheless, it fundamentally altered the electrocatalytic activity of $Co_x(GSH)_y$ as shown by the cathodically shifted CV in the first fraction collected. These results are consistent with the catalytically active form of $Co_x(GSH)_y$ being a labile, multimeric complex. Both monomeric 1:1 Co(GSH) and multimeric $Co_x(GSH)_y$ complexes have been reported previously at neutral and basic pH values, with evidence that complex formation is influenced by variables like pH and metal-to-ligand ratios.[18, 22, 23] Unfortunately, the instability of this complex precludes its isolation and detailed characterization.

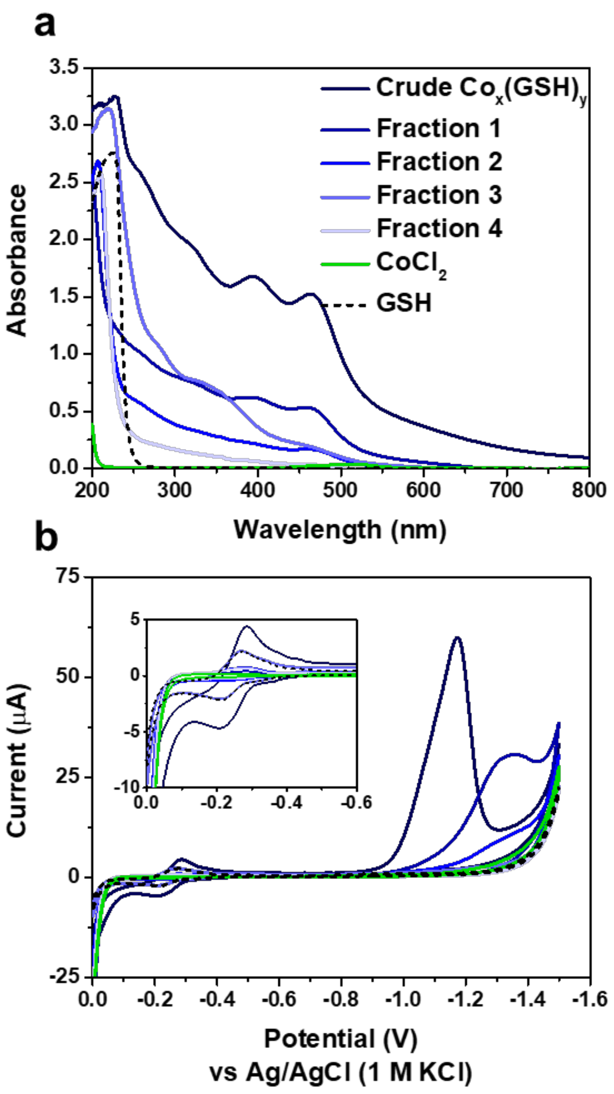

**Figure 3.** (a) Absorbance spectra of $Co_x(GSH)_y$ before and after column purification. Fractions 1-4 refer to the fractions collected from the P2 size-exclusion column. (b) CVs (100 mV/s) of the corresponding $Co_x(GSH)_y$ samples in 0.5 M AA/1 M KCl in water, pH 4.5, with a hanging mercury drop working electrode, Ag/AgCl (1 M KCl) reference electrode, and Pt wire counter electrode. For both the crude sample, which was lyophilized and dissolved in ~1 mL of water, and fractions 1-4, which are more dilute in comparison, exact concentrations are unknown. The inset highlights the region from 0 to –0.6 V. The redox feature near –0.3 V for both $Co_x(GSH)_y$ and GSH, arises from the GSH/GSSG redox couple. $Co_x(GSH)_y$ was prepared with 6.7 mM $Co^{2+}$ rather than the 1 uM $Co^{2+}$ used in catalysis to ensure adequate signal.

We similarly attempted to characterize the catalyst formed in the CdSe-MPA system. Combining $CoCl_2$ and MPA in a 1:2 ratio at pH 4.5, a deep-brown product with absorption maxima at 370 and 457 nm was formed (Figure S10). The absorption features of this *in situ* generated $Co_x(MPA)_y$ species resemble those observed upon complexation of cobalt with GSH (*vide*

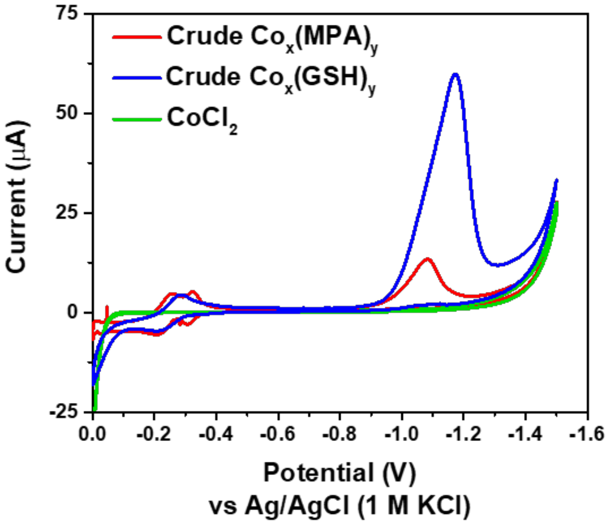

**Figure 4.** CVs (100 mV/s) of the crude $Co_x(GSH)_y$ and $Co_x(GSH)_y$ samples in 0.5 M AA/1 M KCl in water, pH 4.5, with a hanging mercury drop working electrode, Ag/AgCl (1 M KCl) reference electrode, and Pt wire counter electrode. $Co_x(GSH)_y$ was prepared with 6.7 mM $Co^{2+}$ rather than the 1 uM $Co^{2+}$ used in catalysis to ensure adequate signal.

*supra*). As with crude $Co_x(GSH)_y$, the CV of $Co_x(MPA)_y$ exhibits an irreversible wave, consistent with proton reduction, with an onset potential of ~-0.9 V (Figure 4). This feature is not observed in samples containing only $CoCl_2$ or MPA. Again, these results suggest that the electrochemical feature arises from a $Co_x(MPA)_y$ complex. We again attempted to purify the catalyst through size-exclusion chromatography but observed the complete loss of the electrocatalytic activity observed in the crude sample, indicating that the catalytically active form of $Co_x(MPA)_y$ is labile (Figure S10). Although the electrochemical activity was quenched, fractions collected nevertheless exhibited the characteristic absorption bands seen in the crude sample and also seen in $Co_x(GSH)_y$ indicating presence of a cobalt-MPA complex.

The similarities between the absorption spectra and CVs of the crude samples of $Co_x(GSH)_y$ and $Co_x(MPA)_y$ suggests that the thiol and/or carboxylic acid moieties are responsible for catalytic activity of both species. Interestingly, we observe a five-fold higher catalytic current for $Co_x(GSH)_y$ than for $Co_x(MPA)_y$, indicating that $Co_x(GSH)_y$ has higher electrocatalytic activity for $H_2$ production. This difference could be due to the amine groups of GSH, which have been shown to act as proton shuttles in other catalysts.[24] In addition, the higher stability of $Co_x(GSH)_y$, evidenced by the residual activity of the first column fraction, may enhance its activity relative to $Co_x(MPA)_y$. We, therefore, assign the difference in $H_2$ production for the photochemical CdSe-GSH and CdSe-MPA systems in the presence of $Co^{2+}$ (figure 2) to this distinction in the activity of these catalysts that form *in situ*.

Here, we report a robust photocatalytic system with CdSe QDs and a molecular cobalt catalyst formed *in situ* from a simple cobalt salt and a ubiquitous biomolecule, GSH. This robust photocatalytic system has high efficiency and activity (TON of 210,000 over 91 hrs). Proton reduction by the catalyst occurs near –0.9 V (with respect to vs. Ag/AgCl (1 M KCl)), which is consistent with the potential needed to accept a photoelectron from the CdSe QD. Planned work aiming to gain a more detailed understanding of the catalytically active complex(es) will move us toward a rational design of new proton reduction catalysts and cooperative QD-catalyst interactions. This work is supported by the Chemical Sciences, Geosciences and Biosciences Division, Office of Basic Energy Sciences, Office of Science, U.S. Department of Energy, Grant No. DE-FG02-09ER16121.

## Conflicts of interest

There are no conflicts to declare.

## Notes and references

1 K. L. Bren, *Interface Focus*, 2015, **5**, 20140091.
2 Z. Han and R. Eisenberg, *Acc. Chem. Res.*, 2014, **47**, 2537.
3 J. Jasieniak, M. Califano and S. E. Watkins, *ACS Nano*, 2011, **5**, 5888.
4 A. P. Alivisatos, *J Phys Chem-Us*, 1996, **100**, 13226.
5 M. Bruchez, M. Moronne, P. Gin, S. Weiss and A. P. Alivisatos, *Science*, 1998, **281**, 2013.
6 Z. Han, F. Qiu, R. Eisenberg, P. L. Holland and T. D. Krauss, *Science*, 2012, **338**, 1321.
7 T. Simon, N. Bouchonville, M. J. Berr, A. Vaneski, A. Adrovic, D. Volbers, R. Wyrwich, M. Doblinger, A. S. Susha, A. L. Rogach, F. Jackel, J. K. Stolarczyk and J. Feldmann, *Nat. Mater.*, 2014, **13**, 1013.
8 Y. Ben-Shahar, F. Scotognella, I. Kriegel, L. Moretti, G. Cerullo, E. Rabani and U. Banin, *Nat. Commun.*, 2016, **7**, 10413.
9 A. Das, Z. J. Han, M. G. Haghighi and R. Eisenberg, *Proc. Natl. Acad. Sci. U. S. A.*, 2013, **110**, 16716.
10 K. Han, M. Wang, S. Zhang, S. Wu, Y. Yang and L. Sun, *Chem. Commun.*, 2015, **51**, 7008.
11 J. Huang, K. L. Mulfort, P. Du and L. X. Chen, *J. Am. Chem. Soc.*, 2012, **134**, 16472.
12 C. Gimbert-Suriñach, J. Albero, T. Stoll, J. Fortage, M.-N. Collomb, A. Deronzier, E. Palomares and A. Llobet, *J. Am. Chem. Soc.*, 2014, **136**, 7655.
13 K. A. Brown, M. B. Wilker, M. Boehm, G. Dukovic and P. W. King, *J. Am. Chem. Soc.*, 2012, **134**, 5627.
14 Z.-J. Li, X.-B. Li, J.-J. Wang, S. Yu, C.-B. Li, C.-H. Tung and L.-Z. Wu, *Energy Environ. Sci.*, 2013, **6**, 465.
15 C. M. Chang, K. L. Orchard, B. C. M. Martindale and E. Reisner, *J. Mater. Chem. A*, 2016, **4**, 2856.
16 S. Losse, J. G. Vos and S. Rau, *Coord. Chem. Rev.*, 2010, **254**, 2492.
17 E. H. Edwards, A. A. Fertig, K. P. McClelland, M. T. Meidenbauer, S. Chakraborty, T. D. Krauss, K. L. Bren and E. M. Matson, *Chem. Commun.*, 2020, **56**, 8762.
18 B. K. Singh, R. K. Sharma and B. S. Garg, *Spectrochim. Acta. A*, 2006, **63**, 96.
19 R. G. Neville and G. Gorin, *J. Am. Chem. Soc.*, 1956, **78**, 4891.
20 K. Hori, *B. Chem. Soc. Jpn.*, 1975, **48**, 2209.
21 R. Kizek, J. Vacek, L. Trnkova and F. Jelen, *Bioelectrochemistry*, 2004, **63**, 19.
22 C. Bresson, R. Spezia, P. L. Solar, C. K. Jankowski and C. Den Auwer, *J. Inorg. Biochem.*, 2015, **142**, 126.
23 B. Harman and I. Sovago, *Inorg. Chim. Acta*, 1983, **80**, 75.
24 W. A. Hoffert, J. A. S. Roberts, R. Morris Bullock and M. L. Helm, *Chem. Commun.*, 2013, **49**, 7767.